



## Research article

# Psoralen attenuates cigarette smoke extract-induced inflammation by modulating CD8<sup>+</sup> T lymphocyte recruitment and chemokines via the JAK2/STAT1 signaling pathway

Shi-huan Li<sup>a,1</sup>, Qiu-ping Li<sup>a</sup>, Wen-jing Chen<sup>a</sup>, Yuan-yuan Zhong<sup>a</sup>, Jing Sun<sup>a,c</sup>, Jin-feng Wu<sup>a,b</sup>, Yu-xue Cao<sup>a,c,\*\*</sup>, Jing-cheng Dong<sup>a,c,\*</sup>

<sup>a</sup> Department of Integrative Medicine, Huashan Hospital, Fudan University, Shanghai, 200040, China

<sup>b</sup> Department of Dermatology, Huashan Hospital, Fudan University, Shanghai, 200040, China

<sup>c</sup> Institutes of Integrative Medicine, Fudan University, Shanghai, 200040, China

## ARTICLE INFO

## Keywords:

Psoralen  
COPD  
Inflammation  
T cell recruitment  
Chemokines

## ABSTRACT

Chronic obstructive pulmonary disease (COPD) is a respiratory inflammatory disease. Psoralen (PSO) is the main pharmacological component identified from Bu-Shen-Fang-Chuan formula which has been traditionally used in treatment of COPD, yet its efficacy in COPD inflammation were unreported. In this study, we aimed to elucidate the anti-inflammatory potential of PSO in COPD and unravel the underlying mechanisms, focusing on T lymphocyte recruitment and the modulation of chemokines, namely monokine induced by interferon-gamma (CXCL9), interferon inducible protein 10 (CXCL10), and interferon inducible T-Cell alpha chemoattractant (CXCL11). In vitro, RAW264.7 was stimulated by interferon (IFN)- $\gamma$  + cigarette smoke extract (CSE) and were treated with PSO (2.5, 5, 10  $\mu$ M), then the levels of chemokines and the activation of Janus kinase (JAK)/Signal transducer and activator of transcription 1 (STAT1) pathway were analyzed by real time PCR and western blot. In vivo, a murine model was established by intraperitoneal injection of CSE on day 1, 8, 15, and 22, then treated with PSO (10 mg/kg). Our experiments in vitro illustrated that PSO reduced the levels of CXCL9, CXCL10, and CXCL11, and decreased the protein phosphorylation levels of JAK2 and STAT1. Additionally, PSO effectively improved inflammatory infiltration and decreased the proportion of CD8<sup>+</sup> T cells in CSE-exposed mice. Furthermore, PSO reduced the levels of CXCL9, CXCL10, and CXCL11 in bronchoalveolar lavage fluid (BALF) and lung tissue, and decreased the protein phosphorylation levels of JAK2 and STAT1. In conclusion, our results revealed the therapeutic potential of PSO for COPD inflammation, possibly mediated through the regulation of CD8<sup>+</sup> T cell recruitment and chemokines via the JAK2/STAT1 signaling pathway.

**Abbreviations:** COPD, chronic obstructive pulmonary disease; PSO, psoralen; CSE, cigarettes smoke extract; CXCL9, monokine induced by interferon-gamma; CXCL10, interferon inducible protein 10; CXCL11, interferon inducible T-Cell alpha chemoattractant; IFN, interferon; CXCR3, C-X-C motif chemokine receptor 3; JAK, Janus kinase; STAT1, signal transducer and activator of transcription 1; ELISA, enzyme-linked immunosorbent assay; BALF, bronchoalveolar lavage fluid; GAPDH, glyceraldehyde-3-phosphate dehydrogenase.

\* Corresponding author. Department of Integrative Medicine, Huashan Hospital, Fudan University, Building 6, 3rd floor, Huashan Hospital, No.12, Urumqi Middle Road, Jing'an District, Shanghai, 200040, China.

\*\* Corresponding author. Department of Integrative Medicine, Huashan Hospital, Fudan University, Shanghai, 200040, China.

E-mail address: [jcdong2004@126.com](mailto:jcdong2004@126.com) (J.-c. Dong).

<sup>1</sup> The first author.

<https://doi.org/10.1016/j.heliyon.2024.e32351>

Received 19 October 2023; Received in revised form 1 June 2024; Accepted 3 June 2024

Available online 7 June 2024

2405-8440/© 2024 The Authors. Published by Elsevier Ltd. This is an open access article under the CC BY-NC-ND license (<http://creativecommons.org/licenses/by-nc-nd/4.0/>).

## 1. Introduction

Chronic obstructive pulmonary disease (COPD) is a common condition characterized by chronic airway inflammation and persistent airflow restriction [1]. Cigarette smoke inhalation is one of the leading causes of COPD, and the inflammation induced by cigarette smoke have been the most studied currently [2]. Studies have shown that T lymphocytes (especially CD8<sup>+</sup> T cells) are involved in cigarette smoke-induced inflammation of the lung tissue [3–5], which is closely related to lung tissue damage and progressive decline in lung function [6,7].

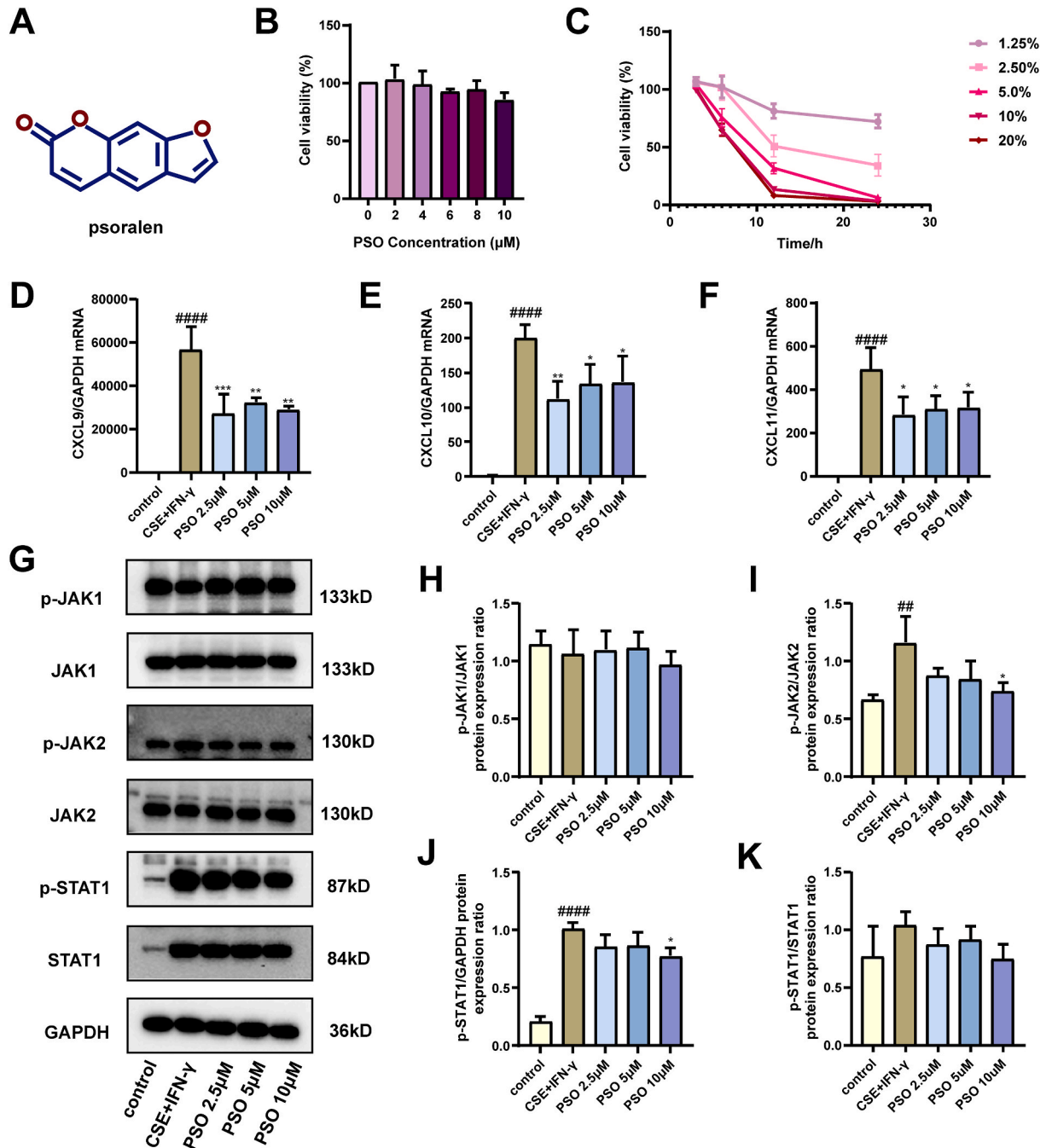


**Fig. 1.** PSO downregulated CXCL9/CXCL10/CXCL11 by inhibiting activation of the JAK2/STAT1 pathway in vitro. (A) The molecular structure of PSO. (B) Effect of PSO on cell viability. (C) Effect of CSE on cell viability. (D–F) Expression of CXCL9/CXCL10/CXCL11 mRNA. (G–K) Expression and quantification of band intensities of the JAK/STAT1 pathway proteins. Data are expressed as mean ± SD (n = 3). ##p < 0.01, ####p < 0.0001 vs. control group; \*p < 0.05, \*\*p < 0.01, \*\*\*p < 0.001 vs. CSE + IFN-γ group.

The migration of T lymphocytes to the inflammatory site in response to inflammatory signals is dependent on chemokines. In patients with COPD, activated T lymphocytes (especially CD8<sup>+</sup> T cells) express chemokine receptors, such as C-X-C motif chemokine receptor 3 (CXCR3), which mainly attracts ligand monokine induced by interferon-gamma (CXCL9), interferon inducible protein 10 (CXCL10), and interferon inducible T-Cell alpha chemoattractant (CXCL11) to migrate to the inflammatory site [8–10]. Moreover, CXCL10 is a biomarker for acute exacerbations of COPD patients [11]. The Janus kinase (JAK)/Signal transducer and activator of transcription (STAT) pathway is a classical signaling pathway involved in the regulation of cytokines and chemokines during inflammatory processes [12]. A study found that activation of the JAK/STAT1 pathway in patients with COPD was significantly increased [13]. In summary, the JAK/STAT1 pathway and CXCL10/CXCR3 chemotaxis may be potential therapeutic targets for COPD treatment.

Traditional Chinese Medicine (TCM) has long been employed in the treatment of COPD due to its considerable clinical efficacy. Our previous study showed that the Bu-Shen-Fang-Chuan formula can effectively inhibit T lymphocyte recruitment in a COPD rat model through suppressing CXCL9/CXCL10/CXCL11-CXCR3 axis and that psoralen (PSO) is the main ingredient of this formula [14,15]. PSO is a principal bioactive component of *Cullen corylifolium* (L) Medik and has been demonstrated to benefit for the treatment of osteoporosis, tumors, and inflammation [16]. Du et al. have reported that PSO exerts therapeutic effects against idiopathic pulmonary fibrosis (IPF) in a bleomycin (BLM)-induced murine model for the first time [17]. Surprisingly, the efficacy of PSO in vivo and in vitro, especially in COPD inflammation, has yet remained unaddressed. Therefore, we aimed to investigate the effect and underlying mechanisms of PSO in a murine model of COPD, and found that PSO was able to markedly attenuate inflammation. Our study provides a novel insight into the regulation of PSO on COPD, and identify potential therapeutic targets for PSO treatment of COPD.

## 2. Materials and methods

### 2.1. Materials and reagents

The 3R4F cigarettes were obtained from the Kentucky Tobacco Research Council (KY, USA). PSO (HPLC  $\geq 98\%$ , the molecular structure was shown in Fig. 1A) was purchased from Shanghai Winherb Medical Technology Co., Ltd., (Shanghai, China). RAW264.7 were obtained from ATCC (TIB-71, USA). RPMI-1640 medium was purchased from KeyGEN Biotech Co., Ltd., (Jiangsu, China). Fetal bovine serum was obtained from Sigma-Aldrich (MO, USA). MTT cell proliferation and cytotoxicity assay kit was obtained from Beyotime Biotechnology Co., Ltd., (Shanghai, China). Recombinant murine interferon (IFN)- $\gamma$  was supplied by PeproTech (NJ, USA). Mouse IFN- $\gamma$ , CXCL9, and CXCL10 enzyme-linked immunosorbent assay (ELISA) kits were purchased from Lianke Biotech Co., Ltd., (Hangzhou, China) and mouse CXCL11 ELISA kit was purchased from Raybiotech (GA, USA). Primary antibodies against CD4, CD8, JAK2, JAK1 (phospho Y1007/1008), and STAT1 (phospho S727) were purchased from Abcam (Kambridge, UK); JAK1 (phospho-Tyr1034/1035) was purchased from Signalway Antibody LLC (MD, USA); JAK1, STAT1, and Glyceraldehyde-3-phosphate dehydrogenase (GAPDH) were purchased from Proteintech (Wuhan, China).

### 2.2. Preparation of CSE and PSO

The CSE used for animal experiments was prepared by collecting a 3R4F cigarette smoke in 2 mL phosphate-buffered saline (PBS) with a peristaltic pump, and for cell experiments was in 10 mL serum-free RPMI-1640 medium, then followed by filtration with a 0.22  $\mu\text{m}$  sterilization filter, which was defined as 100 % CSE [18].

PSO for animal experiments was fully dissolved in dimethyl sulfoxide (DMSO) and diluted in 0.5 % sodium carboxymethyl cellulose (CMC-Na) [19], and for cell experiments was dissolved in DMSO, which the concentration of DMSO in the working solution was not exceed 0.1 %.

### 2.3. Cell viability assay

RAW264.7 were cultured in RPMI-1640 medium containing 10 % (v/v) fetal bovine serum in Thermo Scientific™ Heracell™ 150i (ThermoFisher, USA) with a humidified atmosphere of 5 % CO<sub>2</sub> at 37 °C. When the cells are covered with 80 % of the bottom area, the cell subculture and related experimental operations are performed.

To detect the effect of CSE on cell viability: RAW264.7 ( $1.0 \times 10^5/\text{mL}$ ) were seeded in 96-well plates at 100  $\mu\text{L}/\text{well}$ . After 24 h, 0 %, 1.25 %, 2.5 %, 5 %, 10 %, and 20 % CSE was added to intervene for 3 h, 6 h, 12 h, and 24 h respectively. MTT (the concentration of working solution: 0.5 mg/mL) was added at 10  $\mu\text{L}/\text{well}$  for 3 h, then the medium was discarded and 100  $\mu\text{L}/\text{well}$  DMSO was added and placed on a shaker for 15 min. Optical density (OD) was measured at 490 nm. Cell viability (%) =  $(\text{OD}_{\text{sample}} - \text{OD}_{\text{blank}})/(\text{OD}_{\text{control}} - \text{OD}_{\text{blank}}) \times 100\%$ .

To detect the effect of PSO on cell viability: RAW264.7 ( $1.0 \times 10^5/\text{mL}$ ) were seeded in 96-well plates at 100  $\mu\text{L}/\text{well}$ . After 24 h, cells were treated with different concentrations of PSO (0, 2, 4, 6, 8, 10  $\mu\text{M}$ ) for 24 h. The remaining operations were the same as before.

### 2.4. Cell model and treatments

RAW264.7 ( $1.0 \times 10^5/\text{mL}$ ) were seeded in 6-well plates at a density of 2 mL/well. After 24 h, RAW264.7 were pre-treated with 100  $\mu\text{L}/\text{well}$  CSE (final concentration of 5 %) or not for 3 h, then the medium was aspirated, and the cells were washed with PBS. The cells

were then treated with IFN- $\gamma$  (10 ng/mL) and different concentrations of PSO (2.5, 5, 10  $\mu$ M) or not for 24 h, and the cells were harvested for subsequent detections.

## 2.5. Animal model and treatment

5-week-old male C57BL/6Ncr1 mice (18–20 g) were purchased from Vital River Laboratory Animal Technology Co., Ltd., (Beijing, China) and housed in a specific pathogen free (SPF) room with proper humidity (40 %) and temperature ( $25 \pm 2$  °C), a 12 h light/dark cycle, and free access to distilled water and food. All animal procedures were approved by the Animal Experimentation Ethics Committee of Fudan University (permit number: 2021JS Huashan Hospital-487).

The mice were randomly divided into three groups (n = 10 per group): control, CSE, and CSE + PSO (10 mg/kg). The COPD inflammation mouse model was established by intraperitoneal injection of 0.3 mL CSE on days 1, 8, 15, and 22, and mice in the control group were intraperitoneally injected with 0.3 mL PBS [20]. After the mold was finished, mice in the CSE + PSO group were intragastrically administered with PSO (10 mg/kg, 0.2 mL/d), and the control and CSE groups were treated with 0.5 % CMC-Na containing DMSO (<0.1 %) in the same volume from day 29 to day 35. All the mice were sacrificed on day 36. The operation process was shown in Fig. 2A.

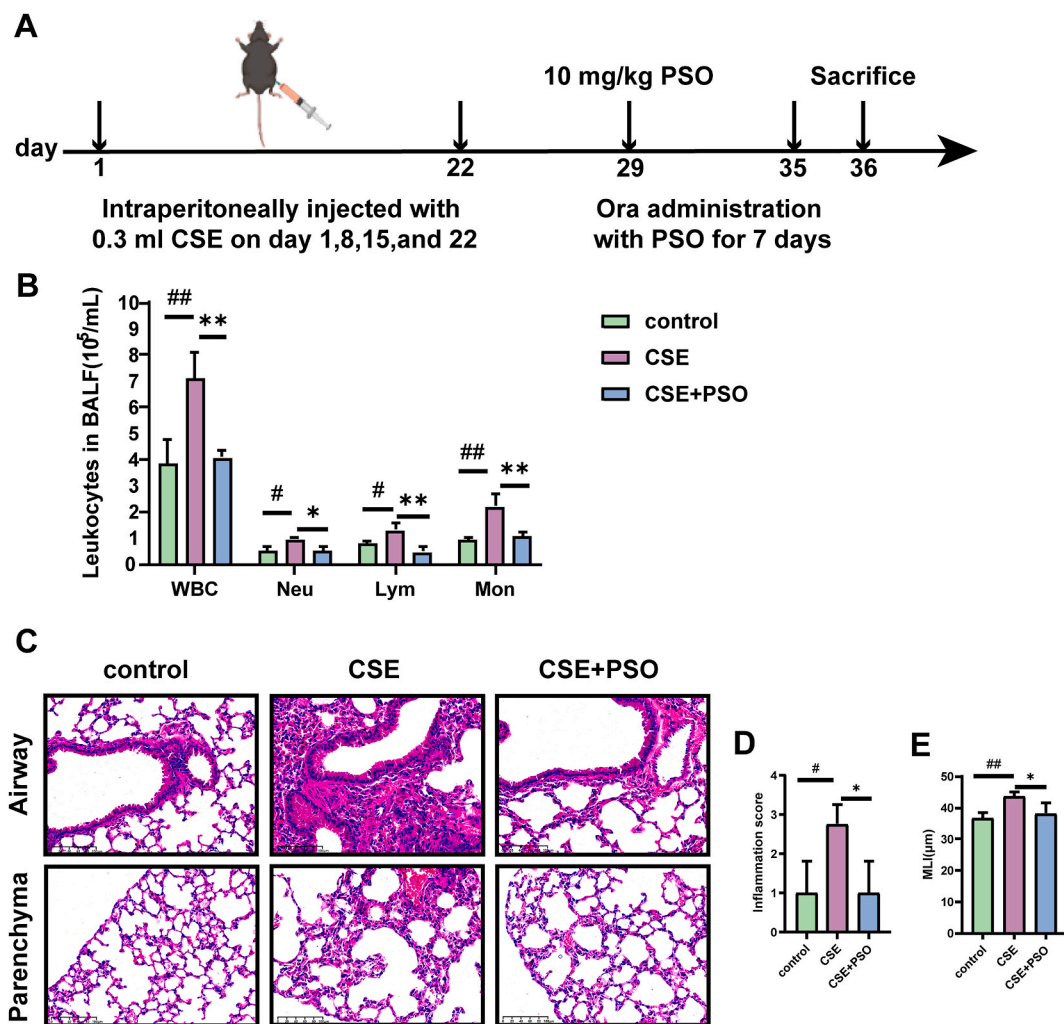


**Fig. 2.** PSO attenuated pulmonary inflammation in CSE-induced mice. (A) Protocol for experimental models had 2 phrases: four times CSE exposed on day 1, 8, 15 and 22 to establish the mold; PSO (10 mg/kg) administration from day 29 to day 35. (B) Total leukocytes, monocytes, lymphocytes, and neutrophils in BALF ( $10^5$ /mL). (C) Representative microphotographs of lung tissue stained with HE (magnification,  $\times 200$ ; scale bar, 100  $\mu$ m). (D) Inflammation score. (E) MLI. Data are expressed as mean  $\pm$  SD (n = 3–4). #p < 0.05, ##p < 0.01 vs. control group; \*p < 0.05, \*\*p < 0.01 vs. CSE group.

## 2.6. Measurement of inflammatory cells in bronchoalveolar lavage fluid (BALF)

The right bronchus of mouse was clipped, and the left lung was lavaged with 0.3 mL pre-cooled PBS three times. After the BALF was centrifuged at 1500 rpm at 4 °C for 10 min, the supernatant was collected and stored at –80 °C, and the cell pellet was resuspended in 100 µL pre-cooled PBS for inflammatory cell counting with a Mindray automatic cell counter (BC-5000 Vet; Shenzhen, China).

## 2.7. HE staining

After BALF was obtained, the right lung was excised and the most complete lobe was fixed with 4 % paraformaldehyde solution for 48 h, embedded in paraffin wax, and cut into 4–6 µm slice for HE staining. Images were obtained using a digital pathological sliced scanner (KF-PRO-120; Zhejiang, China), and the morphological structure and inflammatory infiltration of the lung tissues were evaluated using the inflammation score and mean linear intercept (MLI). 5 random fields were selected in each slice for statistical analysis. The 0–3 grades described by Triantaphyllopoulos et al. was used for the inflammation score [21], which 0 score represents no injury, 1 score represent modest injury, 2 score represent intermediate injury, 3 score represent severe injury. MLI measurements were performed according to the method described by Choe et al. [22].

## 2.8. Immunohistochemical (IHC) analysis

The embedded lung tissue was sliced, dewaxed, rehydrated, and subjected to IHC. Afterwards, the slides were incubated with primary antibodies (against CD8 and CD4) at 4 °C overnight, followed by incubation with secondary antibodies from a suitable species source for 1 h at room temperature. After washing with PBS three times, diaminobenzidine was added and the degree of coloration was controlled using a light microscope. Images were obtained using a digital pathological sliced scanner (KF-PRO-120; Zhejiang, China). For each group, 6 tissue sections were selected and 5 random fields were examined for each section. CD4<sup>+</sup> and CD8<sup>+</sup> T cells in the lung tissues were evaluated using Image Pro Plus software (version6.0; Media Cybernetics, USA).

## 2.9. Real-time PCR analysis

RNA was extracted using a total RNA extraction kit (Jianshi Biotech, Beijing, China) and cDNA was synthesized using Takara Prime Script™ RT Master Mix (Perfect Real Time) (Beijing, China). The reverse transcription conditions were 37 °C for 15 min; 85 °C for 5 s; and held at 4 °C. The real-time PCR reaction system included ABclonal Genious 2X SYBR Green Fast qPCR Mix (Low ROX Premixed) (Wuhan, China), cDNA, and primers (the sequences of the primers are shown in Table 1, which are from the GenBank and validated by NCBI). Afterwards, the reaction plate was placed in a real-time PCR instrument (Quant Studio 6 Flex, ThermoFisher, USA), and the cycling conditions were as follows: pre-denaturation at 95 °C for 3 min, followed by 40 cycles of denaturation at 95 °C for 5 s and annealing at 60 °C for 30 s. GAPDH was chosen as an internal reference, and the expression of target genes was calculated using the comparative CT method ( $2^{-\Delta\Delta Ct}$ ).

## 2.10. ELISA

The concentrations of IFN- $\gamma$ , CXCL9, CXCL10, and CXCL11 in BALF and lung tissue were detected using ELISA kits for mouse IFN- $\gamma$ , CXCL9, CXCL10, and CXCL11, according to the manufacturer's protocols.

## 2.11. Western blot analysis

Total protein from the lung tissue of mice and cells was extracted using RIPA reagent containing a protease/phosphatase inhibitor. After the protein concentration was detected by the BCA method, the protein was separated by 8 % sodium dodecyl sulfate-polyacrylamide gelelectrophoresis (SDS-PAGE) and transferred to 0.45 µm polyvinylidene fluoride (PVDF) membranes. The membranes were then blocked with 5 % skim milk for 1 h at room temperature, followed by incubation with diluted primary antibodies at 4 °C overnight. After washing three times with Tris buffered saline containing 0.1 % Tween 20 (TBST), the membrane was incubated with the appropriate secondary antibody for 1 h on a shaker. After washing three times with TBST, the membranes were visualized using an enhanced chemiluminescence kit (Tanon, Shanghai, China), and images were obtained.

**Table 1**  
The sequences of primers (mouse).

Name	Forward	Reverse
CXCL9	GGAGITCGAGGAACCCTAGTG	GGGATTTGTAGTGGATCGTGC
CXCL10	CCAAGTGCTGCCGTCATTTTC	GGCTCGCAGGGATGATTTCAA
CXCL11	GGCTTCCTTATGTTCAAACAGGG	GCCGTTACTCGGGTAAATTACA
GAPDH	TGACCTCAACTACATGGTCTACA	CTTCCATTCTCGGCCCTTG

## 2.12. Statistical analysis

The data involved in this study are presented as mean  $\pm$  standard deviation (M  $\pm$  SD) and were analyzed using GraphPad Prism 8.0.2 software (GraphPad Software, CA, USA). Differences among groups were evaluated using one-way analysis of variance (ANOVA) followed by Bonferroni's multiple comparison tests. Statistical significance was set at  $p < 0.05$ .

## 3. Results

### 3.1. PSO downregulated CXCL9/CXCL10/CXCL11 in vitro by inhibiting activation of the JAK2/STAT1 pathway

Based on the results of MTT assay (Fig. 1B and C), we pre-treated RAW264.7 with 5 % CSE or not for 3 h, followed by IFN- $\gamma$  (10 ng/mL) and PSO (2.5, 5, 10  $\mu$ M) or not co-cultured for 24 h, and then harvested cells for measurements of the mRNA levels of CXCL9/CXCL10/CXCL11 by real-time PCR. As demonstrated in Fig. 1D–F, the mRNA expression of CXCL9/CXCL10/CXCL11 in the CSE + IFN- $\gamma$  group were significantly increased compared with those in the control group (all  $p < 0.0001$ ), and PSO intervention downregulated the above indicators, illustrating that PSO was capable of downregulating the mRNA expression of CXCL9/CXCL10/CXCL11 in response to CSE + IFN- $\gamma$ .

IFN- $\gamma$ , combined with its receptor, activates the JAK/STAT1 pathway, which mediates the secretion of downstream cytokines and chemokines [23]. To investigate whether PSO inhibited production of CXCL9/CXCL10/CXCL11 is related to the JAK/STAT1 pathway, western blot was used to detect JAK1, JAK2, and STAT1 proteins. As shown in Fig. 1G–K, the protein phosphorylation levels of JAK2

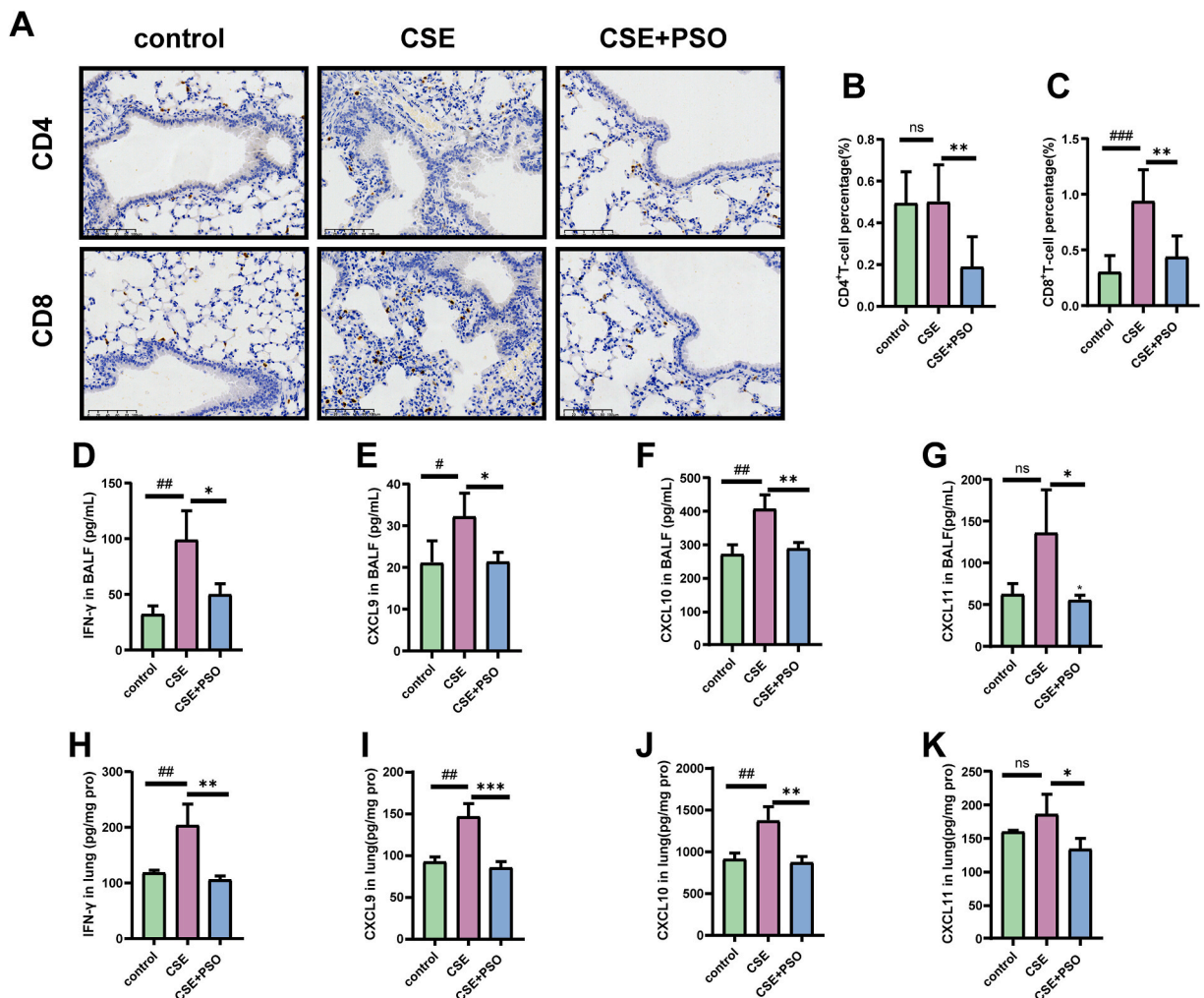


**Fig. 3.** PSO reduced CD8<sup>+</sup> T cell infiltration and chemokine CXCL9/CXCL10/CXCL11 levels in CSE-induced mice. (A) Representative microphotographs of lung tissue in mice with CD4<sup>+</sup> and CD8<sup>+</sup> T cell specific staining (magnification,  $\times 200$ ; scale bar, 100  $\mu$ m). (B) CD4<sup>+</sup> T cell percentages (%). (C) CD8<sup>+</sup> T cell percentages (%). (D–K) Levels of IFN- $\gamma$ , CXCL9, CXCL10, and CXCL11 in BALF and in the lung tissue. Data are expressed as mean  $\pm$  SD ( $n = 3-6$ ). # $p < 0.05$ , ## $p < 0.01$ , ### $p < 0.001$  vs. control group; \* $p < 0.05$ , \*\* $p < 0.01$ , \*\*\* $p < 0.001$  vs. CSE group.

and STAT1 in CSE + IFN- $\gamma$ -stimulated RAW264.7 were remarkably increased, and PSO (10  $\mu$ M) evidently decreased these levels (35.58 % and 23.67 %). Thus, PSO resulted in the decline of CXCL9/CXCL10/CXCL11 in CSE + IFN- $\gamma$ -stimulated RAW264.7 partially may depend on the inhibition of the JAK2/STAT1 pathway.

### 3.2. PSO attenuated pulmonary inflammation induced by CSE in mice

The effects of PSO on CSE-induced pulmonary inflammation in mice were evaluated by detecting inflammatory cells in BALF and pathological staining with HE. As shown in Fig. 2B, PSO administration reduced the numbers of total leukocytes (42.99 %), monocytes (53.03 %), lymphocytes (66.67 %), and neutrophils (46.43 %). HE staining (Fig. 2C) showed that inflammatory infiltration was increased and the alveolar cavity was enlarged in the lung tissue of the CSE group compared with the control group, which were confirmed by the inflammation score (Fig. 2D) and MLI (Fig. 2E), and which in the PSO group were evidently improved. In summary, administration of PSO effectively attenuated pulmonary inflammation in CSE-induced mice.

### 3.3. PSO alleviated CD8<sup>+</sup> T cell infiltration and chemokine CXCL9/CXCL10/CXCL11 levels in CSE-induced mice

Lymphocyte infiltration is a major feature of COPD. To understand the effect of PSO on CSE-induced lymphocyte infiltration, IHC staining was performed. CD8<sup>+</sup> T cell proportion in the lung tissue of the CSE group (Fig. 3A–C) were significantly increased compared with the control group ( $p < 0.001$ ), and treatment with PSO decreased this proportion (0.94 % vs. 0.44 %). At the same time, PSO administration markedly reduced CD4<sup>+</sup> T cell infiltration compared with the CSE group ( $p < 0.01$ ); however, there was no significant difference between the control group and CSE group (Fig. 3A and B). Therefore, PSO alleviated CSE-induced CD8<sup>+</sup> T cell infiltration in the lung tissue of CSE-induced mice.

Lymphocyte chemotaxis requires induction of specific chemokines. we detected the protein levels of IFN- $\gamma$ , CXCL9, CXCL10, and CXCL11 in BALF and lung tissue. As shown in Fig. 3D–K, PSO treatment obviously downregulated the levels of IFN- $\gamma$  (49.62 % and 48.57 %), CXCL9 (33.77 % and 42.13 %), and CXCL10 (29.17 % and 36.73 %) in both BALF and lung tissue. However, in comparison with the control group, the level of CXCL11 protein in the CSE group was increased in BALF but not in lung tissue; PSO decreased the levels of CXCL11 (58.59 % and 28.35 %) in both BALF and lung tissue.

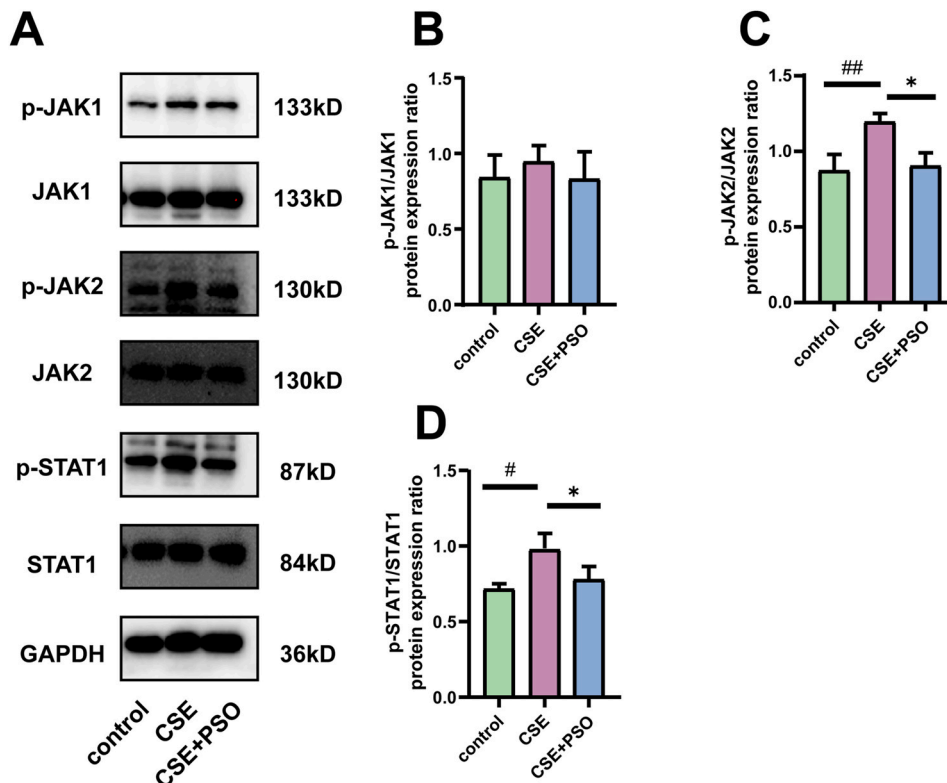


**Fig. 4.** PSO inhibited the activation of JAK2/STAT1 pathway in CSE-induced mice. (A) Proteins expression of the JAK/STAT1 pathway. (B–D) Quantification of band intensities of the JAK/STAT1 pathway proteins. Data are expressed as mean  $\pm$  SD ( $n = 3$ ). # $p < 0.05$ , ## $p < 0.01$  vs. control group; \* $p < 0.05$  vs. CSE group.

### 3.4. PSO reduced activation of the JAK2/STAT1 pathway in CSE-induced mice

To investigate whether the JAK/STAT1 pathway is involved in decreasing the secretion of chemokine CXCL9/CXCL10/CXCL11 after PSO intervention, we detected the activation of this pathway by western blot. The results demonstrated (Fig. 4A–D) that the phosphorylation levels of JAK2 and STAT1 protein in the CSE group were significantly higher than those in the control group ( $p < 0.01$ ,  $p < 0.05$ ), and all decreased after PSO administration (24.56 % and 20.00 %). Compared with the control group, there was no significant difference in the increase in JAK1 protein phosphorylation in the CSE group, and PSO intervention did not change this outcome. Therefore, PSO was capable of reducing activation of the JAK2/STAT1 pathway in CSE-induced mice.

## 4. Discussion

The anti-inflammatory effects of PSO have been supported, especially in autoimmune diseases such as rheumatoid arthritis [16]. PSO is one of the main ingredients of the Bu-Shen-Fang-Chuan formula (used for clinical COPD treatment) [14,15], however, its specific role and underlying mechanisms in COPD management have yet to be elucidated. Chemokine CXCL9/CXCL10/CXCL11, which mediates the chemotaxis of  $CD8^+$  T cell, is secreted by epithelial cells, neutrophils, and macrophages et al. [24–26]. In this study, the cell model was established by  $IFN-\gamma$  + CSE-stimulated RAW264.7 [27], the results illustrated that PSO markedly reduced CXCL9/CXCL10/CXCL11 levels in  $IFN-\gamma$  + CSE-stimulated RAW264.7, and this might be depended on the inhibitory effect on JAK2/STAT1 pathway. However, the JAK/STAT pathway has a negative feedback regulatory mechanism [28,29], therefore, whether PSO works by directly inhibiting the phosphorylation of JAK2 and STAT1 or by indirectly regulating the suppressor of cytokine signaling (SOCS) of the JAK2/STAT1 pathway requires further study.

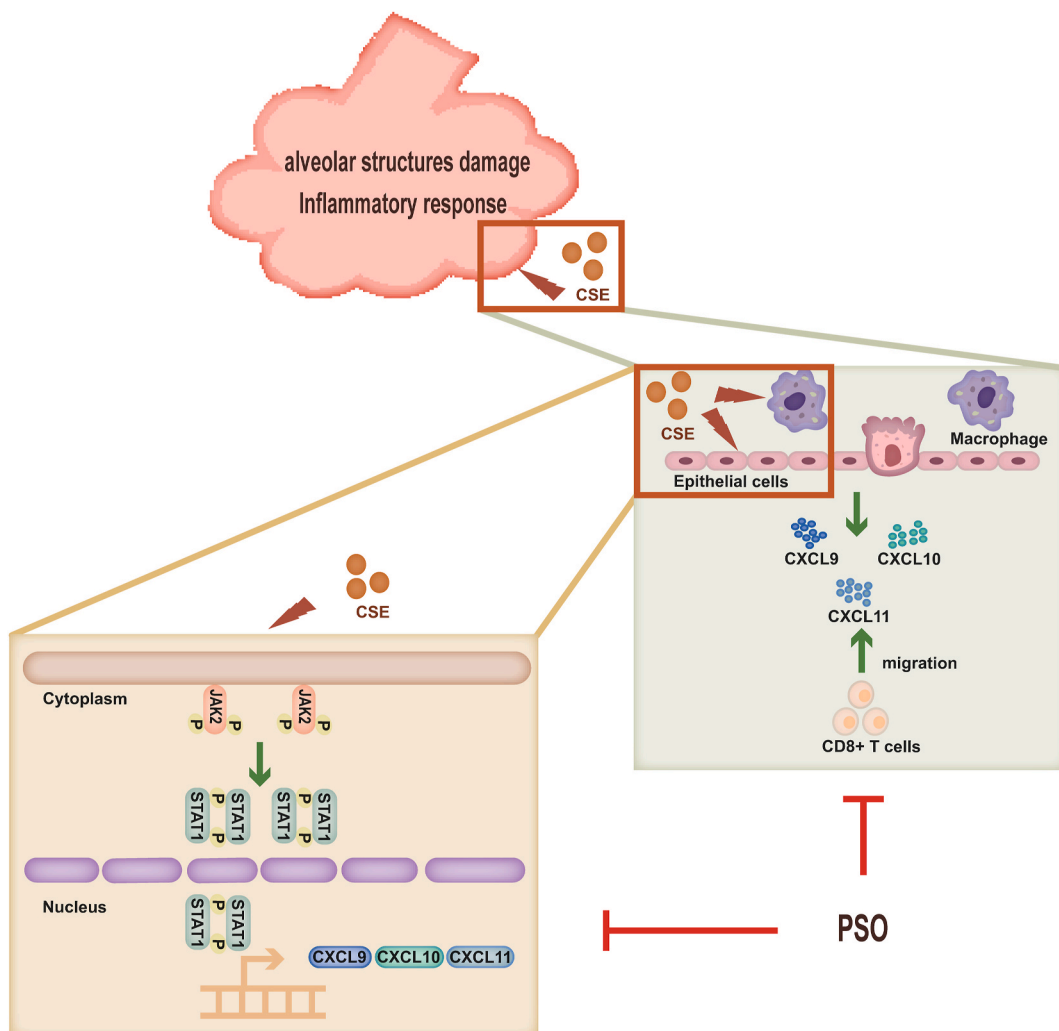


**Fig. 5.** Migration of  $CD8^+$  T cells induced by CXCL9/CXCL10/CXCL11 leads to lung tissue damage and inflammation. PSO attenuates  $CD8^+$  T cell recruitment induced by CSE by suppressing the levels of CXCL9/CXCL10/CXCL11 via the JAK2/STAT1 pathway.

This study further clarifies the therapeutic effects and mechanisms of PSO on the pulmonary inflammation in COPD. We constructed a murine model of COPD inflammation induced via intraperitoneal injection of CSE. Consistent with previous studies [30], intraperitoneal injection of CSE led to an inflammatory response, mainly manifested in an obvious increase in the number of inflammatory cells in BALF (including total leukocytes, monocytes, lymphocytes, and neutrophils), and HE staining showed increased infiltration of inflammatory cells in lung tissue and enhanced alveolar destruction. After PSO intervention, the above situation significantly improved, indicating that PSO inhibited pulmonary inflammation in COPD. CD8<sup>+</sup> T cells mediate inflammatory injury of lung tissue [31], and studies have shown that reducing T lymphocyte infiltration reduces alveolar structural damage in a long-term cigarette smoke exposure mouse model [32]. Therefore, alleviating T lymphocyte infiltration is important for the prevention and treatment of COPD. Our IHC results showed that PSO effectively reduced the infiltration of CD8<sup>+</sup> T cells in the lung tissue of CSE-induced inflammatory mice, indicating that PSO has the effect of reducing CD8<sup>+</sup> T cell infiltration.

CXCL10/CXCR3 chemotaxis is important for mediating CD8<sup>+</sup> T cell migration. Our model of CSE-induced inflammation was consistent with clinical studies and showed elevated CXCL9/CXCL10/CXCL11 levels [10], and PSO reduced the levels of these chemokines, indicating that PSO inhibited CD8<sup>+</sup> T cell infiltration by downregulating CXCL9/CXCL10/CXCL11 levels. In addition, PSO reduced IFN- $\gamma$  levels in mouse BALF and lung tissue in this study. IFN- $\gamma$  is an important inflammatory factor in response to exogenous stimuli (viruses, etc.) and the activation of Th1 type immune responses [33]. IFN- $\gamma$  binds to its receptors to initiate downstream signaling by activating the JAK/STAT1 pathway [34,35]. The JAK/STAT pathway is closely related to the production of chemokines and cytokines, plays an important role in regulating the immune system, and is an important target for the prevention and treatment of inflammatory and autoimmune diseases [36,37]. This experiment showed that PSO inhibited the phosphorylation of JAK2/STAT1 proteins, indicating that PSO inhibited CXCL9/CXCL10/CXCL11 levels, which may depend on the regulation of JAK2/STAT1 pathway activation induced by CSE. In summary, this study showed that CD8<sup>+</sup> T cell migration induced by CXCL9/CXCL10/CXCL11 leads to lung tissue damage and inflammation, and PSO might attenuates CD8<sup>+</sup> T cell recruitment induced by CSE by suppressing the levels of CXCL9/CXCL10/CXCL11 via the JAK2/STAT1 pathway.

However, the infiltration of CD8<sup>+</sup> T cells in lung tissue might not only related to chemotaxis enhancement but also to dysregulation of T cell proliferation and apoptosis. Studies have showed that the progression of COPD includes an autoimmune component, and the dysregulation of T cell proliferation and apoptosis that is antigen dependent is sufficient to cause lung pathology and inflammation [38]. Therefore, further research is needed to explore the role of PSO on proliferation and apoptosis of T lymphocytes in CSE-induced mouse model to bolster the mechanistic explanation. In addition, in the pathological state of chronic inflammation in COPD, monocytes and T lymphocytes further promotes disease progression by cooperating migration towards CXCR3 ligands [39], and which secretion is related with monocytes' response to IFN- $\gamma$  [40]. Therefore, the interaction between inflammatory cells needs to be further clarified to gain a more comprehensive and in-depth understanding of the anti-inflammatory mechanism of PSO in COPD.

## 5. Conclusions

In summary, the present study indicated (Fig. 5) that PSO improves inflammation and alleviates CD8<sup>+</sup> T cell recruitment in CSE-induced mice, probably through attenuating chemokines via the JAK2/STAT1 pathway, which provides theoretical evidence for PSO in the treatment of CSE-induced airway inflammation.

## Declaration

1. Animal procedures were approved by the Animal Experimentation Ethics Committee of Fudan University (permit number: 2021JS Huashan Hospital-487).
2. There are no conflicts of interests.

## Funding sources

This work was funded by the National Natural Science Foundation of China (82104788 and 81973631).

## Data availability statement

The data supporting the findings of this study are available within the supplementary materials.

## CRedit authorship contribution statement

**Shi-huan Li:** Writing – review & editing, Writing – original draft, Data curation. **Qiu-ping Li:** Software, Investigation. **Wen-jing Chen:** Visualization, Formal analysis, Data curation. **Yuan-yuan Zhong:** Visualization, Software. **Jing Sun:** Project administration. **Jin-feng Wu:** Project administration, Methodology. **Yu-xue Cao:** Investigation, Funding acquisition. **Jing-cheng Dong:** Funding acquisition.

## Declaration of competing interest

The authors declare that they have no known competing financial interests or personal relationships that could have appeared to

influence the work reported in this paper.

## Appendix A. Supplementary data

Supplementary data to this article can be found online at <https://doi.org/10.1016/j.heliyon.2024.e32351>.

## References

- [1] W.W. Labaki, S.R. Rosenberg, Chronic obstructive pulmonary disease, *Ann. Intern. Med.* 173 (3) (2020) Itc17–itc32, <https://doi.org/10.7326/aitc202008040>.
- [2] S.A. Christenson, B.M. Smith, M. Bafadhel, et al., Chronic obstructive pulmonary disease, *Lancet* 399 (10342) (2022) 2227–2242, [https://doi.org/10.1016/S0140-6736\(22\)00470-6](https://doi.org/10.1016/S0140-6736(22)00470-6).
- [3] M. Saetta, A. Di Stefano, G. Turato, et al., CD8+ T-lymphocytes in peripheral airways of smokers with chronic obstructive pulmonary disease, *Am. J. Respir. Crit. Care Med.* 157 (3 Pt 1) (1998) 822–826, <https://doi.org/10.1164/ajrccm.157.3.9709027>.
- [4] M. Saetta, Airway inflammation in chronic obstructive pulmonary disease, *Am. J. Respir. Crit. Care Med.* 160 (5 Pt 2) (1999) S17–S20, <https://doi.org/10.1164/ajrccm.160.supplement.1.6>.
- [5] V.I. Peinado, J.A. Barberá, P. Abate, et al., Inflammatory reaction in pulmonary muscular arteries of patients with mild chronic obstructive pulmonary disease, *Am. J. Respir. Crit. Care Med.* 159 (5 Pt 1) (1999) 1605–1611, <https://doi.org/10.1164/ajrccm.159.5.9807059>.
- [6] G. Turato, R. Zuin, M. Miniati, et al., Airway inflammation in severe chronic obstructive pulmonary disease: relationship with lung function and radiologic emphysema, *Am. J. Respir. Crit. Care Med.* 166 (1) (2002) 105–110, <https://doi.org/10.1164/rccm.2111084>.
- [7] M.S. Paats, I.M. Bergen, H.C. Hoogsteden, et al., Systemic CD4+ and CD8+ T-cell cytokine profiles correlate with GOLD stage in stable COPD, *Eur. Respir. J.* 40 (2) (2012) 330–337, <https://doi.org/10.1183/09031936.00079611>.
- [8] S.G. Kelsen, M.O. Aksoy, M. Georgy, et al., Lymphoid follicle cells in chronic obstructive pulmonary disease overexpress the chemokine receptor CXCR3, *Am. J. Respir. Crit. Care Med.* 179 (9) (2009) 799–805, <https://doi.org/10.1164/rccm.200807-10890C>.
- [9] M. Saetta, M. Mariani, P. Panina-Bordignon, et al., Increased expression of the chemokine receptor CXCR3 and its ligand CXCL10 in peripheral airways of smokers with chronic obstructive pulmonary disease, *Am. J. Respir. Crit. Care Med.* 165 (10) (2002) 1404–1409, <https://doi.org/10.1164/rccm.2107139>.
- [10] C. Costa, R. Rufino, S.L. Traves, et al., CXCR3 and CCR5 chemokines in induced sputum from patients with COPD, *Chest* 133 (1) (2008) 26–33, <https://doi.org/10.1378/chest.07-0393>.
- [11] M. Bafadhel, S. McKenna, S. Terry, et al., Acute exacerbations of chronic obstructive pulmonary disease: identification of biologic clusters and their biomarkers, *Am. J. Respir. Crit. Care Med.* 184 (6) (2011) 662–671, <https://doi.org/10.1164/rccm.201104-0597OC>.
- [12] X. Hu, J. Li, M. Fu, et al., The JAK/STAT signaling pathway: from bench to clinic, *Signal Transduct Target Ther* 6 (1) (2021) 402, <https://doi.org/10.1038/s41392-021-00791-1>.
- [13] L. Yew-Booth, M.A. Birrell, M.S. Lau, et al., JAK-STAT pathway activation in COPD, *Eur. Respir. J.* 46 (3) (2015) 843–845, <https://doi.org/10.1183/09031936.00228414>.
- [14] Q. Li, J. Sun, Y. Cao, et al., Bu-Shen-Fang-Chuan formula attenuates T-lymphocytes recruitment in the lung of rats with COPD through suppressing CXCL9/CXCL10/CXCL11-CXCR3 axis, *Biomed. Pharmacother.* 123 (2020) 109735, <https://doi.org/10.1016/j.biopha.2019.109735>.
- [15] Q. Li, G. Wang, S.H. Xiong, et al., Bu-Shen-Fang-Chuan formula attenuates cigarette smoke-induced inflammation by modulating the PI3K/Akt-Nrf2 and NF-κB signalling pathways, *J. Ethnopharmacol.* 261 (2020) 113095, <https://doi.org/10.1016/j.jep.2020.113095>.
- [16] Y. Ren, X. Song, L. Tan, et al., A review of the pharmacological properties of psoralen, *Front. Pharmacol.* 11 (2020) 571535, <https://doi.org/10.3389/fphar.2020.571535>.
- [17] M.Y. Du, J.X. Duan, C.Y. Zhang, et al., Psoralen attenuates bleomycin-induced pulmonary fibrosis in mice through inhibiting myofibroblast activation and collagen deposition, *Cell Biol. Int.* 44 (1) (2020) 98–107, <https://doi.org/10.1002/cbin.11205>.
- [18] Q. Li, J. Sun, N. Mohammadtursun, et al., Curcumin inhibits cigarette smoke-induced inflammation via modulating the PPARγ-NF-κB signaling pathway, *Food Funct.* 10 (12) (2019) 7983–7994, <https://doi.org/10.1039/c9fo02159k>.
- [19] Y. Wang, H. Zhang, J.M. Jiang, et al., Hepatotoxicity induced by psoralen and isopsoralen from *Fructus Psoraleae*: Wistar rats are more vulnerable than ICR mice, *Food Chem. Toxicol.* 125 (2019) 133–140, <https://doi.org/10.1016/j.fct.2018.12.047>.
- [20] D. Morichika, A. Taniguchi, N. Oda, et al., Loss of IL-33 enhances elastase-induced and cigarette smoke extract-induced emphysema in mice, *Respir. Res.* 22 (1) (2021) 150, <https://doi.org/10.1186/s12931-021-01705-z>.
- [21] K. Triantaphyllopoulos, F. Hussain, M. Pinart, et al., A model of chronic inflammation and pulmonary emphysema after multiple ozone exposures in mice, *Am. J. Respir. Lung Cell Mol. Physiol.* 300 (5) (2011) L691–L700, <https://doi.org/10.1152/ajplung.00252.2010>.
- [22] K.H. Choe, L. Taraseviciene-Stewart, R. Scerbavicius, et al., Methylprednisolone causes matrix metalloproteinase-dependent emphysema in adult rats, *Am. J. Respir. Crit. Care Med.* 167 (11) (2003) 1516–1521, <https://doi.org/10.1164/rccm.200210-1207OC>.
- [23] L.B. Ivashkiv, IFNγ: signalling, epigenetics and roles in immunity, metabolism, disease and cancer immunotherapy, *Nat. Rev. Immunol.* 18 (9) (2018) 545–558, <https://doi.org/10.1038/s41577-018-0029-z>.
- [24] A. Sauty, M. Dziejman, R.A. Taha, et al., The T cell-specific CXC chemokines IP-10, Mig, and I-TAC are expressed by activated human bronchial epithelial cells, *J. Immunol.* 162 (6) (1999) 3549–3558.
- [25] S. Gasperini, M. Marchi, F. Calzetti, et al., Gene expression and production of the monokine induced by IFN-gamma (MIG), IFN-inducible T cell alpha chemoattractant (I-TAC), and IFN-gamma-inducible protein-10 (IP-10) chemokines by human neutrophils, *J. Immunol.* 162 (8) (1999) 4928–4937.
- [26] M.Q. Zhao, M.H. Stoler, A.N. Liu, et al., Alveolar epithelial cell chemokine expression triggered by antigen-specific cytolytic CD8(+) T cell recognition, *J. Clin. Invest.* 106 (6) (2000) R49–R58, <https://doi.org/10.1172/jci9786>.
- [27] Q. Li, J. Sun, Y. Cao, et al., Icaritin inhibited cigarette smoke extract-induced CD8(+) T cell chemotaxis enhancement by targeting the CXCL10/CXCR3 axis and TGF-β/Smad2 signaling, *Phytomedicine* 96 (2022) 153907, <https://doi.org/10.1016/j.phymed.2021.153907>.
- [28] J.J. O'Shea, P.J. Murray, Cytokine signaling modules in inflammatory responses, *Immunity* 28 (4) (2008) 477–487, <https://doi.org/10.1016/j.immuni.2008.03.002>.
- [29] G.A. Durham, J.J.L. Williams, M.T. Nasim, et al., Targeting SOCS proteins to control JAK-STAT signalling in disease, *Trends Pharmacol. Sci.* 40 (5) (2019) 298–308, <https://doi.org/10.1016/j.tips.2019.03.001>.
- [30] L. Lin, G. Hou, D. Han, et al., Ursolic acid protected lung of rats from damage induced by cigarette smoke extract, *Front. Pharmacol.* 10 (2019) 700, <https://doi.org/10.3389/fphar.2019.00700>.
- [31] R.I. Enelow, A.Z. Mohammed, M.H. Stoler, et al., Structural and functional consequences of alveolar cell recognition by CD8(+) T lymphocytes in experimental lung disease, *J. Clin. Invest.* 102 (9) (1998) 1653–1661, <https://doi.org/10.1172/jci4174>.
- [32] P.L. Podolin, J.P. Foley, D.C. Carpenter, et al., T cell depletion protects against alveolar destruction due to chronic cigarette smoke exposure in mice, *Am. J. Physiol. Lung Cell Mol. Physiol.* 304 (5) (2013) L312–L323, <https://doi.org/10.1152/ajplung.00152.2012>.
- [33] M. Majori, M. Corradi, A. Caminati, et al., Predominant TH1 cytokine pattern in peripheral blood from subjects with chronic obstructive pulmonary disease, *J. Allergy Clin. Immunol.* 103 (3 Pt 1) (1999) 458–462, [https://doi.org/10.1016/S0091-6749\(99\)70471-9](https://doi.org/10.1016/S0091-6749(99)70471-9).

- [34] J.E. Darnell Jr., I.M. Kerr, G.R. Stark, Jak-STAT pathways and transcriptional activation in response to IFNs and other extracellular signaling proteins, *Science* 264 (5164) (1994) 1415–1421, <https://doi.org/10.1126/science.8197455>.
- [35] D.J. Gough, D.E. Levy, R.W. Johnstone, et al., IFN $\gamma$  signaling—does it mean JAK-STAT? *Cytokine Growth Factor Rev.* 19 (5–6) (2008) 383–394, <https://doi.org/10.1016/j.cytogfr.2008.08.004>.
- [36] S. Banerjee, A. Biehl, M. Gadina, et al., JAK-STAT signaling as a target for inflammatory and autoimmune diseases: current and future prospects, *Drugs* 77 (5) (2017) 521–546, <https://doi.org/10.1007/s40265-017-0701-9>.
- [37] A.V. Villarino, Y. Kanno, J.J. O’Shea, Mechanisms and consequences of Jak-STAT signaling in the immune system, *Nat. Immunol.* 18 (4) (2017) 374–384, <https://doi.org/10.1038/ni.3691>.
- [38] B.L. Eppert, B.W. Wortham, J.L. Flury, et al., Functional characterization of T cell populations in a mouse model of chronic obstructive pulmonary disease, *J. Immunol.* 190 (3) (2013) 1331–1340, <https://doi.org/10.4049/jimmunol.1202442>.
- [39] C. Costa, S.L. Traves, S.J. Tudhope, et al., Enhanced monocyte migration to CXCR3 and CCR5 chemokines in COPD, *Eur. Respir. J.* 47 (4) (2016) 1093–1102, <https://doi.org/10.1183/13993003.01642-2015>.
- [40] M. Torvinen, H. Campwala, I. Kilty, The role of IFN- $\gamma$  in regulation of IFN- $\gamma$ -inducible protein 10 (IP-10) expression in lung epithelial cell and peripheral blood mononuclear cell co-cultures, *Respir. Res.* 8 (1) (2007) 80, <https://doi.org/10.1186/1465-9921-8-80>.